Continental J. Applied Sciences
Ojemeri et al. (2024) 19 (2): 111 – 126 Doi: 10.5281/zenodo.14525941

Research Article

Impact of Suction/Injection on Magnetized Free Convection Affected by Thermal Property: A Numerical Approach

Godwin Ojemeri[1*], A. S. Ibrahim[2], Abdulsalam Shuiabu[3] and Abubakar Muhammad Tsafe[4]
[1,3]Department of Mathematics, College of Sciences, Federal University of Agriculture, Zuru, P. M. B. 28, Kebbi State.
[2]Department of Mathematics, Faculty of Sciences, Sokoto State University, Sokoto State.
[4]Department of Mathematics, Faculty of Physical and Computing Sciences, Usmanu Danfodiyo University, P. M. B. 2346, Sokoto.
***Corresponding author: godwinojemeri@gmail.com**

Abstract

In boundary layer control, especially in engineering, aerodynamics, space research, and medicine, suction/injection factors are very crucial. These advantages prompted our interest to dig further into the effect of wall porosity in industrial working fluids. Therefore, this paper analyses unsteady magnetized flow through an upstanding plate with the involvement of suction/injection flow, buoyancy force and temperature dependent thermal property. The nonlinear partial differential equations for momentum and energy are modelled using a semi implicit finite difference scheme, while the analytical equations of the steady-state equations were calculated employing the regular perturbation technique. The solutions obtained were presented and discussed in detail using various line graphs. It is concluded that the injection parameter promotes fluid velocity, while higher suction and magnetic parameters values lead to a drastic reduction in fluid movement respectively. The findings from this research would be helpful for controlling fluid flow in vertical channels as well as aiding the addition and removal of reactants during chemical reactions.

Keywords: Free convection, Buoyancy force parameter, Magnetohydrodynamics (MHD), Suction/injection, Variable thermal conductivity, implicit finite difference scheme.

Received: 20 August 2024 **Accepted: 10 December 2024**

Citation: Ojemeri, G, Ibrahim, A. S., Shuiabu, A., and Tsafe, A.M. (2024). Impact of Suction/Injection on Magnetized Free Convection Affected by Thermal Property: A Numerical Approach. Continental J. Applied Science, 19(2), 111-126. Doi: 10.5281/zenodo.14525941

ISSN: 3043–6087. Science and Education Development Inst., Nigeria

Introduction

The study of electrically conductive liquids, including plasma, electrolytes, salt water, and liquid metals, is called magnetohydrodynamics (MHD). There are numerous technical and commercial applications for this type of liquid, including magnetic drug targeting, crystal formation, power generation, reactor cooling, and MHD sensors (Jawad et al. 2021). Hartmann and Lazarus (1937) were the first to conduct an experimental study of modern MHD flow in laboratories. This research laid the groundwork for the creation of numerous MHD devices, including MHD pumps, MHD generators, brakes, flow meters, and geothermal powered energy extraction. Since then, many works have been published to investigate the impacts of MHD on free convection through various flow channels. To this end, Onwubuya *et al.* (2024) recently simulated the impact of MHD Casson fluid affected by porosity and thermal radiation factors along a permeable channel in an oscillating system. Again, Omokhuale *et al.* (2024) emphasized the function of viscous dissipation on heat and mass flow driven by nanoparticles through a boundary layer cavity in an oscillating system, while Usman *et al.* (2024) demonstrated the effect of thermophoresis on MHD oscillatory flow equipped with nano elements across a boundary layer regime. Ojemeri and Onwubuya (2023) investigated the consequences of viscous dissipation and porosity effects on MHD free convection flow of an incompressible fluid traveling along a slit microchannel that is alternately heated and equipped with superhydrophobic slip and temperature conditions. In another related work, Onwubuya and Ojemeri (2023) performed a comparative analysis of MHD mixed convection with thermal radiation factor in an upstanding porous channel using homotopy perturbation approach. Hamza *et al.* (2023) explained the impact of hydromagnetic natural convection flow on a chemically reacting fluid affected by symmetric and asymmetric heating conditions using the homotopy perturbation technique. Jha *et al.* (2023) echoed the significance of the buoyancy-induced magnetic field flow of a fluid in an upright channel having point or line heat generation or absorption at various channel positions. Hydromagnetic Casson nanofluidic flow for mass and heat transport through a stretching plate was studied by Saeed and Gul (2021). Ojemeri et al. (2023) deliberated on the hydromagnetic flux of an electrically conducting non-Newtonian liquid instigated by the radiative factor in an upright porous channel. References like Hamza et al. (2023), Obalalu et al. (2021), Ojemeri and Hamza (2022 and Hamza et al. (2023) shed more light on this phenomenon

Thermal conductivity has been assumed to be constant in some previously published works. However, it is well known that temperature variations can substantially alter the physical features of the fluid. The fluctuation of thermal conductivity with temperature must be put into consideration so as to accurately envisage flow behavior and heat transfer rate. Thermal characteristics, in particular, thermal diffusivity and conductivity, are crucial bedrock material parameters that regulate heat transmission and temperature increases in the repository zone (Ajibade and Kabir 2020). Variable thermophysical fluid characteristics are therefore crucial for improving fluid heat transmission. The heat transport system is noticeably impacted by temperature-dependent thermal conductivity and viscosity. Several published works on steady flow with varying thermal conductivity are available. Salawu et al. (2021) took this into account when modeling the natural convection flow of a sliding upright channel, which is approximated by the Boussinesq approximation for the buoyancy force and variable thermal conductivity. They reported that a temperature difference in the device facilitates heat transfer and fluid flow. The consequence of temperature-dependent variable thermal conductivity in natural convection under the control of a uniform magnetic field has been investigated by Hamza et al. (2015). An isothermal upstanding plate is immersed in a thermally conductive liquid, and the impacts of different viscosities and thermal conductivities on the natural MHD convection across the plate are studied by Pradip et al. (2021). Carreau cross fluids provoked by variable thermal radiation and thermal conductivity factors were solved by Salahuddin and Awais (2022). The magneto-hydrodynamic Carreau flow was investigated by Abbas et al. (2020) utilizing the homotopy approach with variable fluid parameters. The functions of thermal radiation and viscous dissipation on natural convective fluid were investigated by Nalivale et al. (2022). Carreau liquid with heat flux and thermal property affected by the radiation effect was proposed by Megahed et al. (2019). In their study on heat sources and sinks, Irfan et al. (2018) generalized Fourier's law to be affected by the actions of different thermal conductivities in the Carreau liquid flow. Ewis (2021) carefully studied the impacts of variable thermal conductivity, Darcy number, and Grashof number on heat transfer and free convection in viscoelastic fluids. In their article, Hamza et al. (2022) echoed the significance of steady-state mixed convection along a microchannel whose plates are believed to be affected by momentum slip and energy jump effects. Other works that investigated the applications of this concept include Haque et al. (2015), Bandita (2017) and Pantokratoras (2017).

Processes such as heating, ventilation, and air conditioning (HVAC), antifreeze or heat exchange fluid flows in a nuclear reactor, and heat transfer composition have recently grown significantly to maximize efficiency. These developments have been made possible by the use of improved working fluids, novel channel walls with enhanced heat insulation features, or inventive geometric designs. Therefore, the study of fluid suction or injection flow is of crucial importance for medical sciences as well as technical applications such as the cooling and drying of paper and textiles and the extrusion of metals and polymers, to name a few. It is used in particular for problems with blood circulation, blood flow, cancer treatment, aerodynamics, and other things. Hence, the motivation for this study. To study the analytical and numerical effects of suction and injection on the transient flow of a viscous and electrically conductive fluid having thermal properties and buoyancy under the influence of slip flow conditions, a novel mathematical model is developed in the present study as an extension of the work by Hamza et al. (2015). The displayed line graphs have been used to examine the consequences of important control parameters embedded in the flow configuration. In addition, when comparing the numerical solution and the steady-state solution over a longer period, a high level of agreement was shown, confirming the accuracy and precision of the current analysis.

Mathematical Analysis

Envisage the unsteady free convection flow of an electrically conducting fluid in the involvement of suction/injection, gliding flow, and a transversely applied magnetic field of intensity B_0, within two upstanding plates. It is initially thought that the liquid and the walls are at rest and have the same temperature T'm

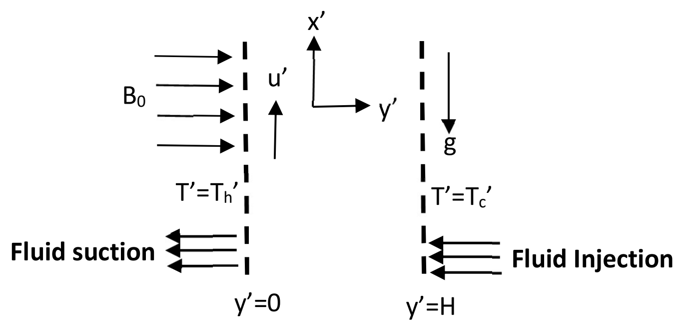

The temperature of the walls is immediately increased or decreased to T'_h or T'_c, respectively, at time t' > 0, so that $T'_h > T'_c$ holds, which is thereafter maintained to be constant. As shown in Figure 1, we have chosen a Cartesian coordinate system where the x-axis is vertical and the y-axis is normal to it. The thermal conductivity (kf) of the liquid is thought to be to changing linearly with temperature in the form $kf = km\,[1 + \delta\,(T' - T'm)]$, see Elbarbary and Elgazery (2004), where km is the free-flow heat of the liquid is conductivity and δ is a constant that varies with the properties of the fluid, with $\delta > 0$ for fluids namely water and air and $\delta < 0$ for fluids such as lubricating oils Elbarbary and Elgazery (2004). According to Hamza et al. (2015) and Boussinesq's approximation, the modelled partial differential equations can be expressed in dimensional form as:

$$\frac{\partial u'}{\partial t'} = V_0 \frac{\partial u'}{\partial y'} + \upsilon \frac{\partial^2 u'}{\partial y'^2} + g\beta (T' - T'_m) - \frac{\sigma B_0^2 u'}{\rho} \tag{1}$$

$$\frac{\partial T'}{\partial t'} = V_0 \frac{\partial T'}{\partial y'} + \frac{1}{\rho c_p}\frac{\partial}{\partial y'}\left[k_f \frac{\partial T'}{\partial y'}\right] \tag{2}$$

The initial and boundary conditions of the current investigation are as follows:

$t' \le 0$: $u' = 0$, $T' = T'_m$, for $0 \le y' \le H$,
$t' > 0$: $u' = 0$, $T' = T'_h$, at $y' = 0$,
$u' = 0$, $T' = T'_c$, at $y' = H$. (3)

To resolve eqns (1) to (3), we apply the following nondimensional variables

$$y = \frac{y'}{H}, \qquad t = \frac{t'\nu}{H^2}, \qquad U = \frac{u'\nu}{g\beta(T_h' - T_m')H^2}, \quad M^2 = \frac{\sigma B_0^2 H^2}{\nu\rho}, S = \frac{V_0 L}{\nu},$$

$$\Pr = \frac{\nu\rho c_p}{k_m}, \qquad \theta = \frac{T' - T_m'}{T_h' - T_m'}, \qquad R = \frac{T_c' - T_m'}{T_h' - T_m'}, \qquad \lambda = \delta(T_h' - T_m')$$

Using eqn (4) on eqns (1) to (3) yield the following:

$$\frac{\partial U}{\partial t} - S\frac{\partial u}{\partial y} = \frac{\partial^2 U}{\partial y^2} - M^2 U + \theta \tag{5}$$

$$\Pr\left[\frac{\partial \theta}{\partial t} - S\frac{\partial \theta}{\partial y}\right] = (1+\lambda\theta)\frac{\partial^2 \theta}{\partial y^2} + \lambda\left[\frac{\partial \theta}{\partial y}\right]^2 \tag{6}$$

The initial and boundary conditions in the dimensionless form are

t<0: $U = 0$, $\theta = 0$, $0 < y < 1$
t>0: (0) =0, θ (0)= 1
(1) = 0, $\theta(1)=R$. (7)

Method of Solution
Regular Perturbation Method
The approximations played an important role in the validation and study of computational solutions to challenging problems. Due to the non-linearity of this problem, we transform the governing equations into a state that can be determined analytically. Substituting $\partial u/\partial t = 0$, and $\partial\theta/\partial t = 0$ into eqns (5) and (6), we get

$$\frac{d^2U}{dy^2} + S\frac{dU}{dy} - M^2U + \theta = 0 \tag{8}$$

$$(1+\lambda\theta)\frac{d^2\theta}{dy^2} + S\Pr\frac{d\theta}{dy} + \lambda\left[\frac{d\theta}{dy}\right]^2 = 0 \tag{9}$$

The boundary conditions are
(0) = 0, θ (0)= 1
(1) = 0, $\theta(1)=R$. (10)

We used a regular perturbation technique in the variable thermal conductivity parameter λ to create an approximate solution to (8) and (9) restricted to (10):

$$\left.\begin{aligned} \theta &= \theta_0 + \lambda\theta_1 \\ U &= U_0 + \lambda U_1 \end{aligned}\right\} \tag{11}$$

inserting eqn (11) into eqns (8) to (10), the solutions of the velocity and temperature equations are derived as:

ISSN: 3043–6087. Science and Education Development Inst., Nigeria

$$\theta = Q_1 + Q_2 e^{-S\Pr y} + \lambda\left[Q_3 + Q_4 e^{-S\Pr y} + Q_1 Q_2 S\Pr y e^{-S\Pr y} - Q_2^2 e^{-2S\Pr y}\right] \tag{12}$$

$$U = Q_5 e^{r1y} + Q_6 e^{-r2y} + Q_7 + Q_8 e^{-S\Pr y} + \lambda\begin{bmatrix} Q_9 e^{r1y} + Q_{10} e^{-r2y} + Q_{11} + Q_{12} e^{-S\Pr y} + Q_{13} y e^{-S\Pr y} \\ +Q_{14} e^{-2S\Pr y} \end{bmatrix} \tag{13}$$

The Nusselt number and skin friction have been calculated as follows:

$$\left.\frac{d\theta}{dy}\right|_{y=0} = -Q_2 S\Pr + \lambda\left[-Q_4 S\Pr + Q_1 Q_2 SPr + 2Q_2^2\right] \tag{14}$$

$$\left.\frac{d\theta}{dy}\right|_{y=1} = -Q_2 S\Pr e^{-S\Pr} + \lambda\begin{bmatrix} -Q_4 S\Pr e^{-S\Pr} + Q_1 Q_2 SPre^{-S\Pr} - Q_1 Q_2 (S\Pr)^2 e^{-S\Pr} \\ +2Q_2^2 e^{-2S\Pr} \end{bmatrix} \tag{15}$$

$$\left.\frac{dU}{dy}\right|_{y=0} = r1Q_5 - r2Q_6 - Q_7 S\Pr + \lambda\left[r1Q_9 - r2Q_{10} - Q_{12} S\Pr + Q_{13} - 2S\Pr\right] \tag{16}$$

$$\left.\frac{dU}{dy}\right|_{y=1} = r1Q_5 e^{r1} - r2Q_6 e^{-r2} - Q_8 S\Pr e^{-S\Pr} + \lambda\begin{bmatrix} r1Q_9 e^{r1} - r2Q_{10} e^{-r2} - Q_{12} S\Pr e^{-S\Pr} \\ +Q_{13} e^{-S\Pr} \end{bmatrix} \tag{17}$$
$$-Q_{13} S\Pr e^{-S\Pr} - 2S\Pr e^{-2S\Pr} \quad]$$

The constants used are all indicated in the appendix section

Numerical Solution

The semi-implicit finite difference approach is employed for the numerical solution of the time-dependent equations (5-7). The forward difference formulas were applied to all time derivatives, and the central difference formula was used to approximate the spatial derivatives. The semi-implicit finite difference equations associated with equations (5-7) are as follows:

$$-r1U_{j-1}^{i+1} + \left[1 + 2r1\right]U_j^{i+1} - r1U_{j+1}^{i+1} = \left[1 - M^2\Delta t\right]U_j^i + r2\left[U_{j+1}^i - U_{j-1}^i\right] + \Delta t\theta_j^i \tag{18}$$

$$-r\theta_{j-1}^{i+1} + \left[\Pr + 2r\right]\theta_j^{i+1} - r\theta_{j+1}^{i+1} = \Pr\theta_j^i + r2\Pr\left[\theta_{j+1}^i - \theta_{j-1}^i\right] + r3\left[\theta_{j+1}^i - \theta_{j-1}^i\right]^2 \tag{19}$$

The boundary conditions are:

$$\left.\begin{array}{ll} U_j^i = 0, & \theta_j^i = 1, \ \ y = 0 \\ U_N^i = 0, & \theta_N^i = R, \ \ y = 1 \end{array}\right\} \tag{20}$$

Where $r = \dfrac{\Delta t\left(1+\lambda\theta_j^i\right)}{\left(\Delta y\right)^2}$, $r1 = \dfrac{\Delta t}{\left(\Delta y\right)^2}$, $r2 = \dfrac{S\Delta t}{2\Delta y}$, $r3 = \dfrac{\lambda \Delta t}{4\left(\Delta y\right)^2}$

The semi-implicit finite difference scheme is unconditionally stable (works for any time step size) and convergent (Makinde and Chinyoka, 2010).

Results and Discussion

The suction/injection parameter (S), Prandtl number (Pr), the magnetic number (M), the variable thermal conductivity parameter (λ), and the buoyancy force distribution parameter (R) are the non-dimensional parameters that control the flow configuration. The analytical and numerical results for momentum, energy, frictional factor, and heat transfer rate for major pertinent parameters dictating the flow are presented graphically. To ascertain the precision and correctness of the numerical approach, the approximate solutions described in the previous section are used. The numerical findings for momentum and energy are compared to the approximations to ensure the accuracy of the system. It is interesting to report that the numerical results of the momentum and energy distributions derived in equations (12) and (13) agree well with the numerical values of the velocity and temperature deduced from equation (18) at the unsteady state time as depicted in figure 2. Further, Figure 3 showcases the relationship between the work of Hamza et al. (2015) and the current work when S = 0. The comparison portrays an excellent relationship at steady state time.

The functions of the suction and injection parameters (S) and the dimensionless time (t) on the temperature and velocity distributions for the cases (i.e. R = 0 and R = 1), respectively, are shown in Figures (4a and b) and figure (5a and b). It is evident that increasing the injection parameter S is seen to drastically improve the fluid velocity while raising the suction parameter is observed to produce the opposite effect. Additionally, the impact of varying thermal property parameter (λ) and time(t) for the both cases for temperature and velocity profiles is noticed to be strengthened until a steady-state time is attained. This is understandable since increasing values improves the energy difference between the outer region of the plate and the surrounding of the boundary layer according to the relationship $\lambda = \delta\left(T_h^{'} - T_m^{'}\right)$. According to Elbarbary and Elgazery (2004), this results in heat moving swiftly from a plate to a liquid inside the boundary layer. Because of this, the gradients of both momentum and energy increased. It implies that as λ grows, so do the fluid flow and the thermal boundary layer thickness.

Figures 6a and b show the pattern of fluid motion for varying values of the magnetic parameter (M) and non-dimensional time (t) on the temperature and velocity distributions for the asymmetric and symmetric cases. According to Figure 6a, the fluid velocity is highest in the region near the heated wall (y = 0) and steadily weakens as it flows towards the cold plate (y = 1). Figure 6 makes it evident that for all considered values of M, there is a symmetrical flow between the walls and that the figures have a parabolic shape. Additionally, it is obvious that rising values of M oppose the flow velocity along the channel surfaces in both Figures 6a and b. The availability of a magnetic effect creates a resistivity force (the Lorentz force) that restrains velocity and is the fundamental cause of this behavior.

Figures 7a-d describe the response of the suction/injection parameter (S) on the variable thermal conductivity λ to the heat transfer rate for non-dimensional time in asymmetric and symmetric cases. It can be seen from the figures that increasing the injection parameter and time t weakens the heat transfer rate at the plate (y = 0), while at higher values of the suction parameters, in both cases, an inverse effect occurs until a steady state is reached. Similarly, the implications of varying the suction/injection parameter (S) versus λ on the skin friction are showcased in Figures 8a–d for a non-dimensional time at R = 0 and R = 1, respectively. As expected, there is a stronger frictional force as the suction parameter and time are increased. However, a contrast behavior is established for rising values of the injection factor.

The sheer stress response in favor of magnetic parameter for ascending values of time at the plates $y = 0$ and $y = 1$ is elucidated in Figure 9a–d for $R = 0$ and R = 1. These figures portray that the drag force diminishes as M and t grow in asymmetric cases, as shown in 9a and b. Figures 9c and d are sketched to illustrate the actions of M on the drag force at the both plates for R = 1. It is noticeable that the skin friction decays as M grows.

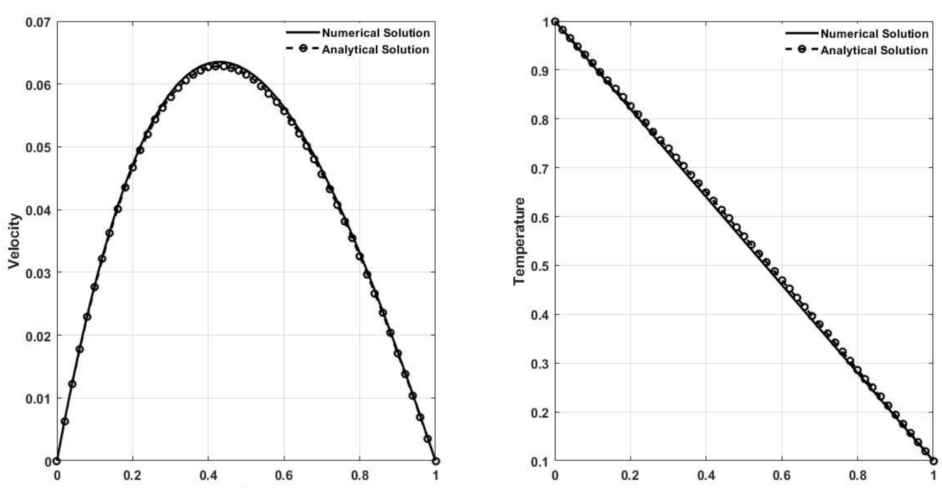

Figure 2: Graphs of numerical solutions and analytical solutions for (a) Velocity and (b) Temperature gradients.

ISSN: 3043–6087. Science and Education Development Inst., Nigeria

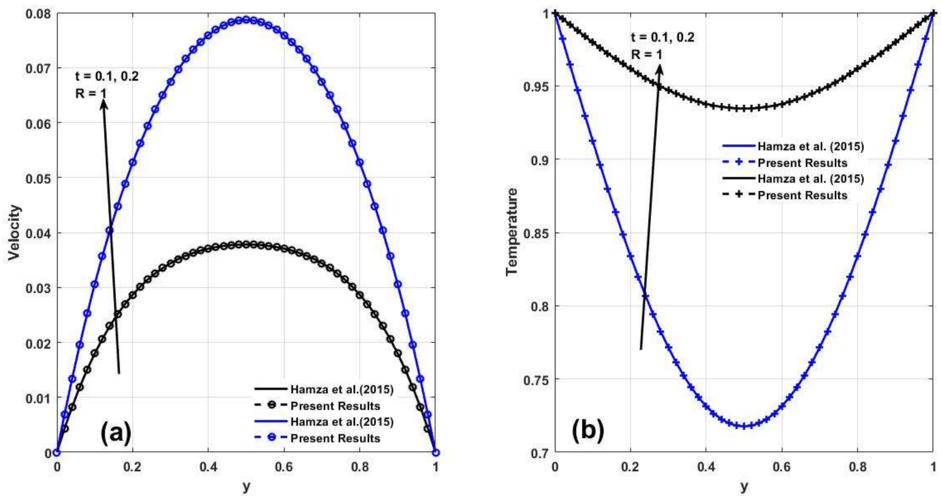

Figure 3: Comparison of Hamza *et al.* (2015) with the present results for the numerical solutions and the approximated solutions at R=1, t=0.1 and 0.2

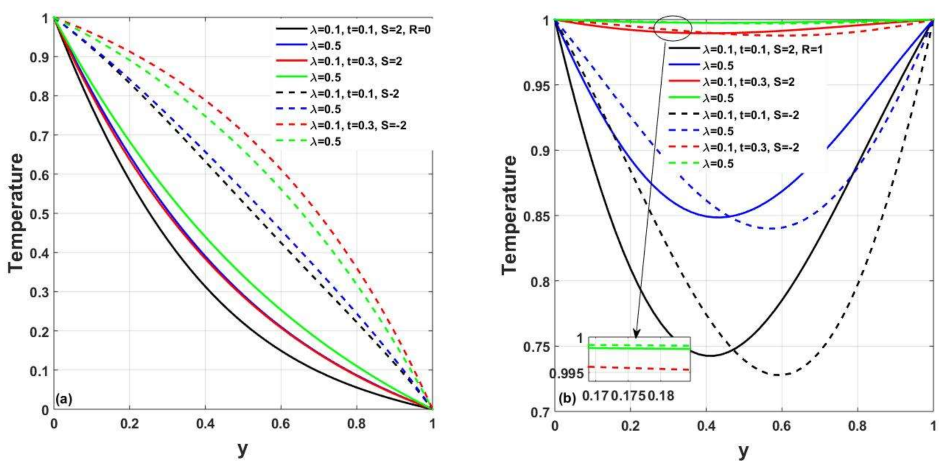

Figure 4: Demonstration of S, λ and time t on unsteady temperature gradient at (a) R=0 and (b) R=1

ISSN: 3043–6087. Science and Education Development Inst., Nigeria

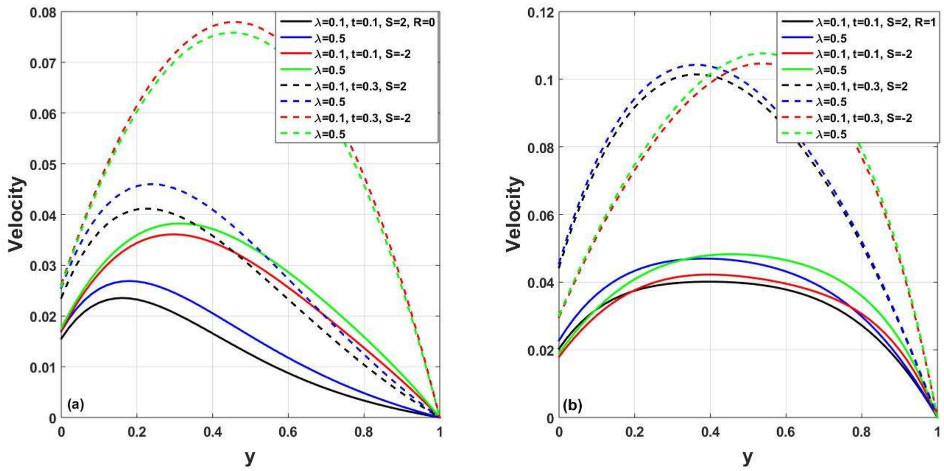

Figure 5: Demonstration of S, λ and time t on unsteady velocity gradient for constant value of Γ at (a) R=0 and (b) R=1

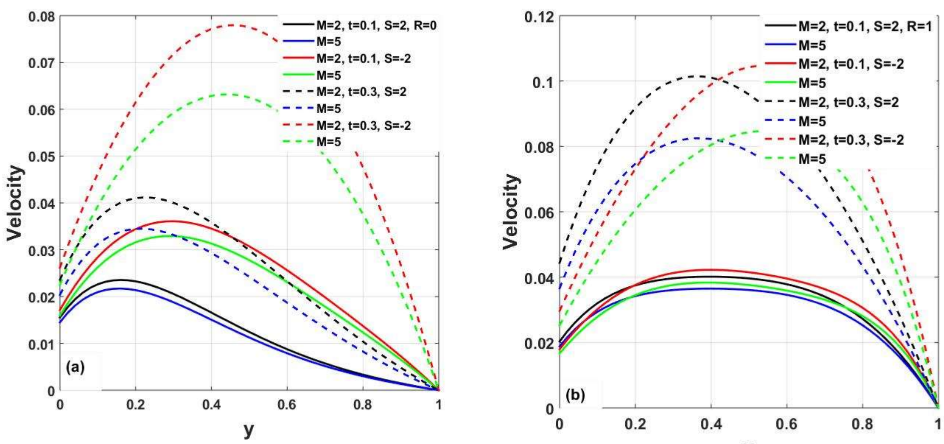

Figure 6: Demonstration of S, M and time t on unsteady velocity gradient for constant values of Pr at (a) R=0 and (b) R=1

ISSN: 3043–6087. Science and Education Development Inst., Nigeria

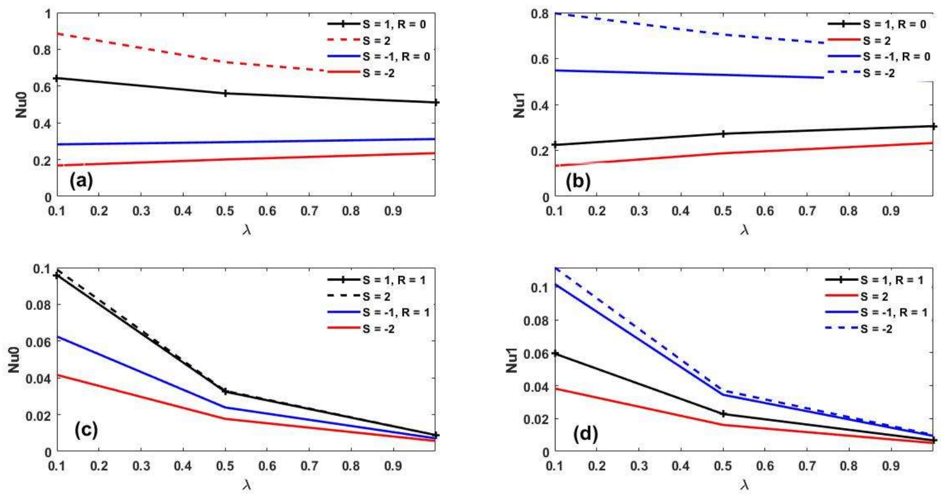

Figure 7: Demonstration of unsteady and steady state Nusselt number versus λ for varying values of S and R at y=0 and y=1

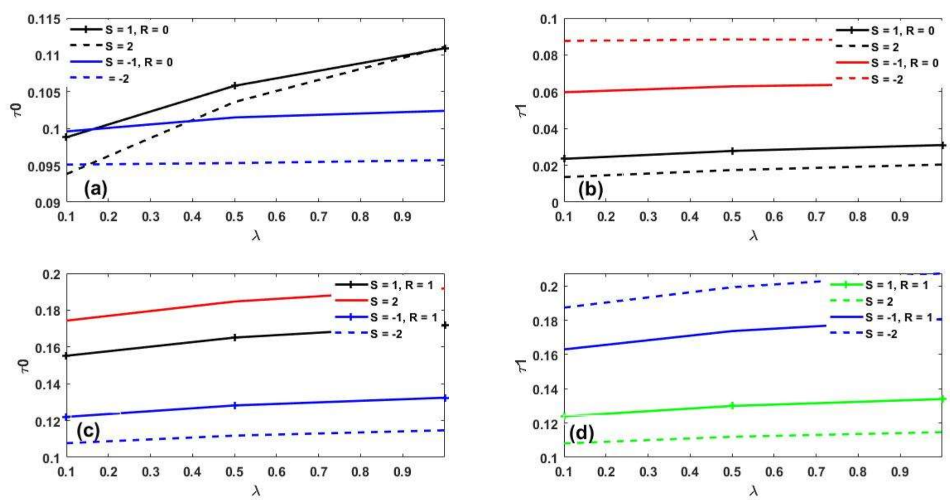

Figure 8: Demonstration of unsteady and steady state Skin friction versus λ for varying values of S and R at y=0 and y=1

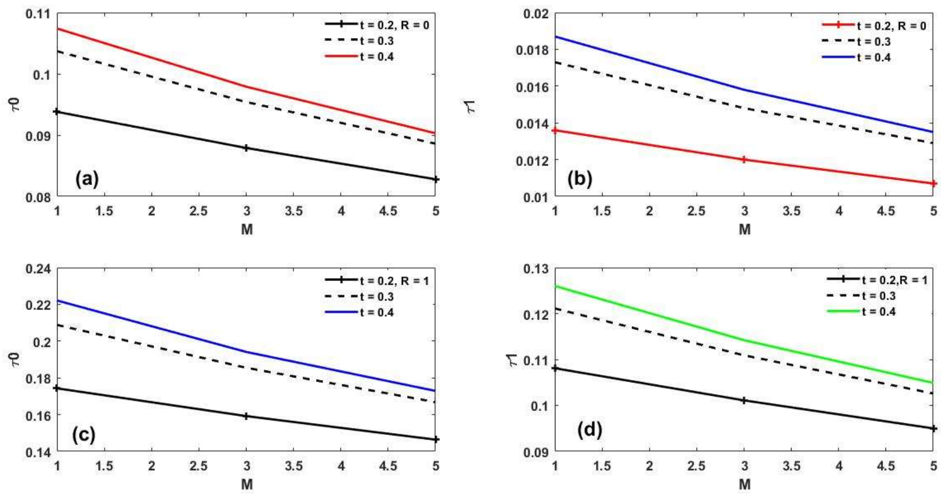

Figure 9: Demonstration of unsteady and steady state Skin friction against M for different values of t and R at y=0 and y=1

Conclusion

The analysis of unsteady and steady hydro-magnetic free convection of an incompressible and electrically conductive fluid flowing through two upright plates with asymmetric and symmetric temperatures on the channel's surface in the coexistence of suction/injection has been investigated with the involvement of thermal property and a uniformly imposed magnetic field. The approximate and numerical solutions of the formulated partial differential equations have been derived employing the regular perturbation technique and the semi-implicit finite difference scheme, respectively. The highlights of the key findings are summarized below:

i. The thermal and velocity flow gradients are seen to be opposed/encouraged for mounting values of suction/injection and nondimensional time for both asymmetric and symmetric cases.
ii. It is revealed that fluid motion and temperature are encouraged with mounting levels of thermal property and nondimensional time for both asymmetric and symmetric heating conditions.
iii. Uplifting the magnetic number lowers the fluid motion, but raising the nondimensional time encourages the velocity for both R = 0 and R = 1.
iv. The heat transfer amount and sheer stress are discovered to be boosted for growing values of the injection parameter at the plate (y = 0), but the converse behavior occurs at y =1 when fluid suction is raised.
v. Skin friction is a growing function of the slip parameter at both plates due to symmetric heating conditions.
vi. In the future, this work will be extended to consider the effects of slip, porous medium and mixed convection

ISSN: 3043–6087. Science and Education Development Inst., Nigeria

Appendix

$$Q_1 = 1-\frac{R-1}{e^{-S\Pr}-1}, \qquad Q_2 = \frac{R-1}{e^{-S\Pr}-1},\ Q_3 = Q_2^2 - Q_4, Q_4 = \frac{Q_2^2 e^{-2S\Pr} - Q_1 Q_2 S \Pr e^{-S\Pr} - Q_2^2}{e^{-S\Pr}-1}$$

$$r1 = \frac{-S+\sqrt{S^2+4M^2}}{2}, r2 = \frac{S+\sqrt{S^2+4M^2}}{2},\ Q_8 = \frac{-Q_2}{\left[S\Pr^2 - S^2\Pr - M^2\right]}, \qquad Q_7 = \frac{Q_1}{M^2}$$

$$s1 = s2 = 1, \qquad s3 = Q_5 s1 + Q_6 s2, \qquad Q_5 = \frac{-s3e^{-r1} - s2Q_7 - s2Q_8 e^{-S\Pr}}{s2e^{r1} - s1e^{-r2}}$$

$$Q_6 = \frac{s3 - Q_5 s1}{s2}, \qquad Q_{11} = \frac{Q_3}{M^2}, \qquad Q_{10} = \frac{p3 - Q_9 p1}{p2}, \qquad Q_{12} = \frac{-Q_4}{S\Pr^2 - S^2\Pr - M^2},$$

$$Q_{13} = \frac{-Q_1 Q_2 S\Pr}{\left[S\Pr^2 - S^2\Pr - M^2\right]}, \qquad Q_{14} = \frac{Q_2^2}{4S\Pr^2 - 2S^2\Pr - M^2}, p1 = p2 = 1,$$

$$p3 = -Q_{11} - Q_{12} - Q_{14},\ Q_9 = \frac{-p3e^{-r2} - p2Q_{14} - p2Q_{12}e^{-S\Pr} - p2Q_{13}e^{-2S\Pr}}{p2e^{r1} - p1e^{-r2}},$$

Nomenclature

B_0 = Magnetic flux density [kg/s^2.m^2]
g= Force due to gravity [m/s^2]
H= Width of the channel [m]
C_pC_v= Specific heats at constant pressure and constant volume [Jkg^{-1}K^{-1}]
λ= Dimensionless variable thermal conductivity
R= Buoyancy force parameter
K= Darcy number
Gre= Mixed convection parameter
γ =Pressure gradient
M= Magnetic field
S=Suction/injection parameter
Pr = Prandlt number
Nu= Heat transfer rate (non-dimensional)
T= Temperature of the fluid (non-dimensional) [K]
T_0=Reference temperature [K]
T_∞^* = The temperature far away from the plate K
U = Velocity of the fluid (non-dimensional) [ms^{-1}]
y= Distance between plates
U_0= Reference velocity [ms^{-1}]
β = Coefficient of thermal expansion [K^{-1}]
μ = Variable fluid viscosity [kgm^{-1}s^{-1}]
k= Thermal conductivity [m.kg/s^3.K]
α = Diffusivity of the Thermal gradient [m^{2}s^{-1}]

σ = Fluid's electrical conductivity [s^3m^2/kg]
ρ = Fluid density [kgm^{-3}]
ν = Kinematic viscosity of the fluid[m^2s^{-1}]

References

Abbas T., Rehman S., Shah R. A., Idrees M. and Qayyum M. (2020). Analysis of MHD Carreau fluid flow over a stretching permeable sheet with variable viscosity and thermal conductivity", *Phys. A*, **551**, 124225.

Ajibade A. O. and Kabir T. M. (2020). The Combined Effect of Variable Viscosity and Variable Thermal Conductivity on Natural Convection Couette Flow. International Journal of Thermofluids. https://doi.org/10.1016/j.ijft.2020.100036.

Bandita P. (2017). Effects of variable viscosity and thermal conductivity on steady MHD slip flow of micropolar fluid over a vertical plate" *Int. J. Comp. Appl. Tech. Res.*, 6(7), pp. 293-298.

Elbarbary E. M. E. and Elgazery E. (2004) Chebyshev finite difference method for the effects of variable viscosity and variable thermal conductivity on heat transfer from moving surfaces with radiation, *Int. J. Ther Sci,* **43**(9), pp.889–899, 2004.

Ewis K. M. (2021). Effects of variable thermal conductivity and Grashof number on non-Darcian natural convection flow of viscoelastic fluids with non-linear radiation and dissipation, *J. Adv. Res. Appl. Sci. Eng. Tech.*, **22** (1).

Hamza M. M., Bello I., Mustapha A., Usman U. and G. Ojemeri (2023). Determining the role of thermal radiation on hydro-magnetic flow in a vertical porous superhydrophobic microchannel, *Dutse J. Pure Applied Sci,* 9(2b), pp. 297-308.

Hamza M. M., Ojemeri G. and Ahmad S. K. (2023). Insights into an analytical simulation of a natural convection flow controlled by Arrhenius kinetics in a micro-channel, *Heliyon* 9, e17628, pp. 1-13, 2023.

Hamza M. M., Shuaibu A. and Ahmad S. K. (2022). Unsteady MHD free convection flow of an exothermic fluid in a convectively heated vertical channel filled with porous medium, *Scientific Reports,* **12**, 11989.

Hamza M. M., Usman I. G. and Sule A. (2015). Unsteady/steady hydromagnetic convective flow between two vertical walls in the presence of variable thermal conductivity", *Journal of fluids,* volume 2015, Article ID:358053

Hamza, M. M., Abdullahi, U., Ahmad, S. K., Omokhuale, E. (2022). Mixed convection flow in a microchannel in the presence of magnetic field and thermal property, *International Journal of Science for Global Sustainability,* **8**(4). https://doi.org/10.57233/ijsgs.v8i4.366

Haque Md. R., Alam Md. M., Ali M. M. and Karim R. (2015). Effect of viscous dissipation on natural convection flow over a sphere with temperature dependent thermal conductivity in presence of heat generation, *Proc. Eng.* 105, pp. 215-224.

Hartmann J. and Lazarus F. (1937). Hg-dynamics II: theory of laminar flow of electrically conductive liquids in a homogeneous magnetic field, *Matematisk-Fysiske Meddelelser*, 15(7), 1937.

ISSN: 3043–6087. Science and Education Development Inst., Nigeria

Irfan M., Khan M. and Khan W. A. (2018). Interaction between chemical species and generalized Fourier's law on 3D flow of Carreau fluid with variable thermal conductivity and heat sink/source: A numerical approach" *Results Physics*, 10, pp. 107–117.

Jawad M., Saeed A. and Gul T. (2021). Entropy generation for MHD Maxwell nanofluid flow past a porous and stretching surface with Dufour and Soret effects, *Braz. J. Phys,* pp. 1-13. htttps://doi.org/10.1007/s13538-020-00835

Jha B. K., Altine M. M. and Hussaini A. M. (2023). MHD steady natural convection in a vertical porous channel in the presence of point/line heat source/sink: An exact solution, *Heat Transfer, Wiley*, pp. 1-15. DOI: 101002/htj.22903

Makinde O. D. and Chinyoka T. (2011). Numerical study of unsteady hydromagnetic Generalized Couette flow of are active third-grade fluid with asymmetric convective cooling", *Computers and Mathematics with Applications*, 61, pp.1167-1179, doi:10.1016/j.camwa.2010.12.066

Megahed A. M. (2019). Carreau fluid flow due to nonlinearly stretching sheet with thermal radiation, heat flux, and variable conductivity", *Appl. Math. Mech.* 40(11), pp. 1615–1624.

Nalivela N. R., Vempati S. R., Ravindra R. B. and Dharmendar R. Y. (2022). Viscous dissipation and thermal radiation impact on MHD mass transfer natural convective flow over a stretching sheet, *Proc. Inst. Mech. Eng. Part E J. Process Mech. Eng*. 09544089221081339.

Obalalu A. M., Ajala O. A., Adeosun A. T., Akindele A. O., Oladapo O. A. and Olajide O. A. (2021). Significance of variable electrical conductivity on non-Newtonian fluid flow between two vertical plates in the coexistence of Arrhenius energy and exothermic chemical reaction", *Partial Diff. Eqn Appl Math,* 4, 100184, pp. 1-9.

Ojemeri G. and Hamza M. M. (2022). Heat transfer analysis of Arrhenius-controlled free convective hydromagnetic flow with heat generation/absorption effect in a micro-channel", *Alexandria Eng. J.*, **61**, pp. 12797-12811.

Ojemeri G. and Onwubuya I. O. (2023). Significance of viscous dissipation and porosity effects in a heated superhydrophobic microchannel, *Journal of Engineering and Technology (JET),* 14(2), pp. 1-19.

Ojemeri G., Omokhuale E., Hamza M. M., Onwubuya I. O. and Shuaibu A. (2023). A Computational Analysis on Steady MHD Casson Fluid Flow Across a Vertical Porous Channel Affected by Thermal Radiation Effect", *Int. J Sci Glob Sus.,* **9**(1). https://doi.org/ 10.57233/ijsgs.v9i1.393

Omokhuale E., Godwin Ojemeri G., Muhammad A. and Usman H. (2024). Significance of Viscous Dissipation on Hydromagnetic Oscillatory Flow Affected by Nanoparticles Through a Boundary Layer Regime, *International Journal of Development Mathematics*, 1(2), 098 - 113

Onwubuya I. O. and Ojemeri G. (2023). Evaluation of mixed convection-radiation flow of a viscous fluid restricted to a vertical porous channel: A comparative Study", *Caliphate Journal Science and Technology,* 5(3), pp. 1-9.

ISSN: 3043–6087. Science and Education Development Inst., Nigeria

Onwubuya I. O., Ojemeri G. and Gyegwe G. T. (2024) The role of Casson fluid flow in a magnetized oscillatory porous channel with non-uniform wall heating, *African Journal of Mathematics and Statistics Studies*, 7(3), pp. 156-167.

Pantokratoras A. (2017). Effects of variable viscosity and thermal conductivity on steady MHD flow of a micropolar fluid through a specially characterized horizontal channel", *Heat transfer AMSE,* 86(1), pp. 1-13.

Pradip S., Sarker K. and Alam Md. M. (2021). Effect of variable viscosity and thermal conductivity on MHD natural convection flow along a vertical flat plate", *Journal of Advances in Mathematics and Computer Science,* **36** (3) pp. 58-71.

Saeed A. and Gul T. (2021). Bio-convection Casson nano-fluid flow together with Darcy-Forchheimer due to a rotating disk with thermal radiation and Arrhenius activation energy, *SN Applied Science*, **3**, 78.

Salahuddin T. and Awais M. A. (2022). Comparative study of Cross and Carreau fluid models having variable fluid characteristics", *Int. Comm. Heat Mass Transf.* 139, 106431.

Salawu O., Okoya S. S. and Hassan A. R. (2021). On free convection flow of a moving vertical permeable plate with quadratic Boussinesq approximation and variable thermal conductivity", *Heat Transfer Research*, **52** (7).

Usman H, Muhammad A. and Omokhuale E. (2024). Enhancing thermophoresis effect on time-dependent magnetohydrodynamics (MHD) oscillatory boundary layer flow occupied with nanoparticles, *International Journal of Science for global sustainability*, 10(1), 197-207. https://doi.org/10.57233/ijsgs.v10i1.611

ISSN: 3043–6087. Science and Education Development Inst., Nigeria